

## CHAPTER II

### THEORY

#### 2.1 Molecular Sieves

Molecular sieves are porous materials that exhibit selective adsorption properties, it must separate components of a mixture on the basis of molecular size and shape differences.<sup>21</sup> The different classes of molecular sieve materials are their element composition in each type. They can be classified into three main types depending on their pore size as shown in Table 2.1.<sup>19</sup>

**Table 2.1** Classification of porous materials

Class of porous	Pore size (Å)	Examples
Micropores	< 20	zeolites, activated carbon
Mesopores	20 - 500	M41S, pillared layered clays
Macropores	> 500	glasses

##### 2.1.1 Zeolites

Zeolites, a type of molecular sieves, are crystalline aluminosilicates of alkali and alkaline earth metals. A zeolite has a three-dimensional network structure of tetrahedral primary building units of  $[\text{SiO}_4]^{-4}$  or  $[\text{AlO}_4]^{-5}$  as shown in Figures 2.1 and 2.2.

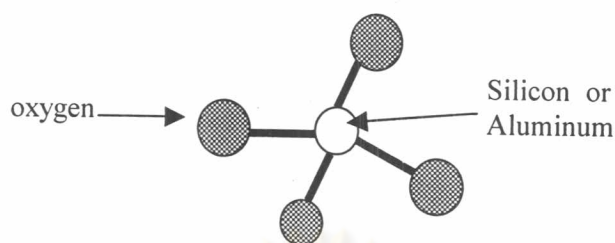


**Figure 2.1** A primary building unit of zeolites

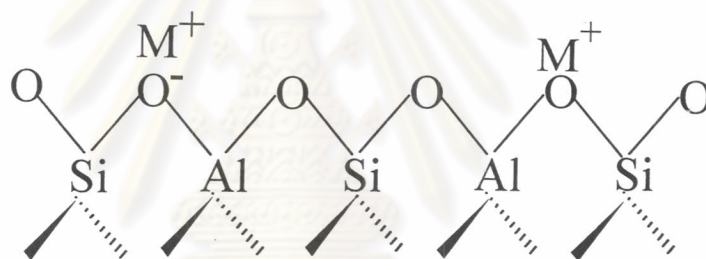
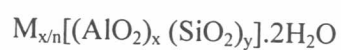


**Figure 2.2** Framework of a zeolite

The tetrahedrons are mutually connected by sharing oxygen atom as shown in Figure 2.2. The negative charge of the lattice is neutralized by the positive charge of the metal cations. In the basic zeolites these are usually cations of univalent and bivalent metals or their combination. A representative unit cell formula for a zeolite is written as:



M represents the exchangeable cations, generally from group IA or IIA in the periodic table of element

$n$  represents the cation oxidation state

$y/x$  is equal to or greater than 2 because  $Al^{+3}$  does not occupy adjacent tetrahedral sites.

Zeolites are crystalline materials. They have a solid framework defining large internal cavities where molecules can be adsorbed. These cavities are interconnected by pore openings through which molecules can pass. Because of their crystalline nature, the pores and cavities are all precisely the same size, and depending on the size of the openings, they can adsorb molecules readily, slowly, or not at all, thus functioning as molecular sieves-adsorbing molecules of certain sizes while rejecting larger ones.

The electrical charge or polarity of the molecules also functions to attract or sort molecules. This ability to selectively adsorb molecules by size and polarity is the key to the unusual efficiency of synthetic zeolites as agents for drying and purifying liquids and gases, and functions as the basis for separation. By tailoring the chemistry and structure of the materials used to create them, synthetic zeolites can be modified to provide a wide range of desired adsorption characteristics or selectivities, and can be used as a separation tool for numerous commercial applications.

### 2.1.2 Shape Selectivity

The pore size and shape in a zeolite may affect the selectivity of a reaction in two ways.<sup>22</sup> (i) *Reactant selectivity* occurs when the aperture size of the zeolite is such that it admits only certain smaller molecules and excludes larger molecules; hence, in a mixture,

effectively only the smaller molecules react. (ii) *Product selectivity* occurs when bulkier product molecules cannot diffuse out, and if formed, they are converted to smaller molecules or to carbonaceous depositing within the pore. (iii) *Transition state selectivity* occur when geometry of intermediate or transition state molecules can not move out of pore. This led to changing the geometry in order to pass to outside of pore. Figure 2.3 shows the models for the three types of selectivity observed in zeolites.

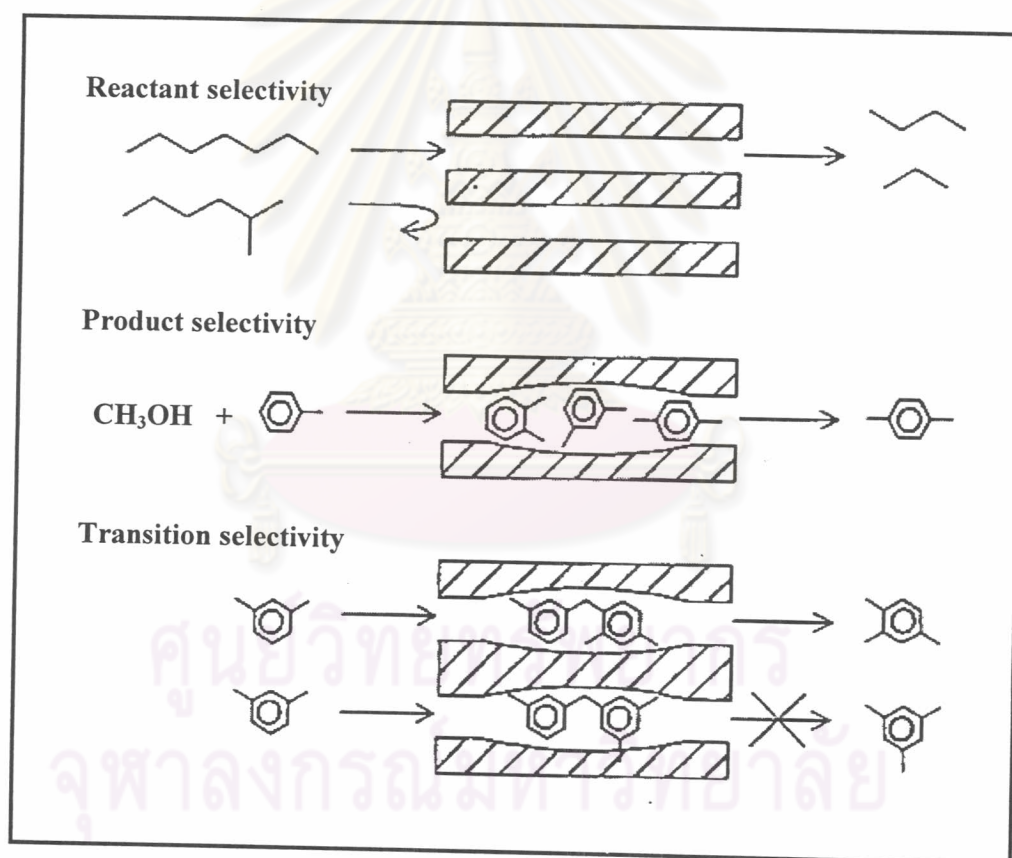


**Figure 2.3** Diagram depicting three types of selectivity: reactant, product and transition-state shape selectivity<sup>21</sup>

### 2.1.3 Mesoporous Materials

Mesoporous materials are member of molecular sieves which have larger pore sizes than microporous zeolite. The utility of these materials is manifested in their microstructures which allow molecules access to large internal surfaces and cavities that enhance catalytic activity and adsorptive capacity. The fundamental breakthrough in this field, marked by the discovery of MCM-41 in 1992 initially precipitated research directed towards. Firstly, the understanding of the formation of ordered mesoporous arrays; secondly, improving the synthetic procedures (aimed at increased efficiency, reproducibility and crystalline quality); and thirdly, functionalisation of the siliceous solids by framework substitution.<sup>23</sup>

#### 2.1.3.1 Characterization of Mesoporous Hexagonal Structure

The X-ray diffraction (XRD) is a reliable technique that can investigate the character of hexagonal mesoporous structure. Typically, the XRD pattern of hexagonal symmetry shows five well-resolved peaks that can be indexed to the corresponding lattice planes of Miller indice (100), (110), (200), (210) and (300). These XRD patterns show at small angle (two theta ( $2\theta$ ) between  $2^\circ$  and  $5^\circ$ ) due to the materials are not crystalline at the atomic level, reflections at higher angles are not observed.

From Bragg's law, when an X-ray beam strikes a crystal surface at some angle  $\theta$ , a portion is scattered by the layer of atoms at the surface. The unscattered portion of the beam penetrates to the second layer of atoms as shown in Figure 2.4, where  $d$  is the interplanar distance of the crystal.<sup>24</sup> Thus, the conditions for constructive interference of the beam at angle  $\theta$  can be described by Bragg equation which is written as equation (2.1).

$$n\lambda = 2d \sin\theta \quad (2.1)$$

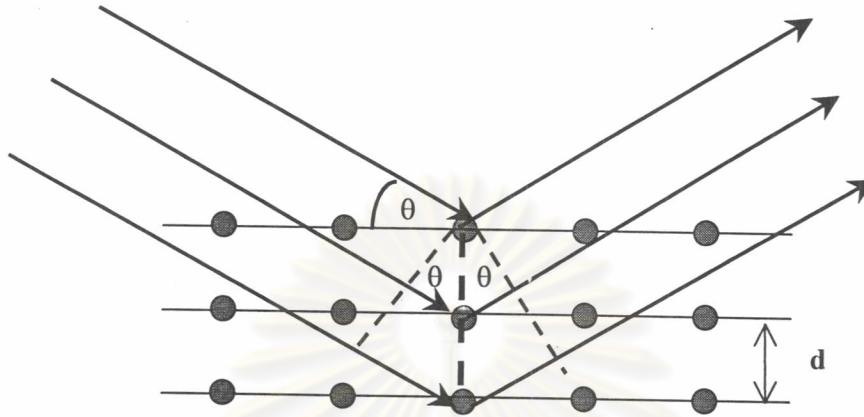


**Figure 2.4** Diffraction of X-ray by a crystal<sup>24</sup>

Hexagonal structure have characteristics of d-spacing ratio as follows :

$$d_{100}/d_{110} = d_{200}/d_{220} = 1.732 = \sqrt{3} \quad (2.2)$$

$$d_{100}/d_{200} = d_{200}/d_{400} = 2.000 \quad (2.3)$$

$$\frac{1}{d^2} = \frac{h^2}{a^2} + \frac{k^2}{b^2} + \frac{l^2}{c^2} \quad (2.4)$$

From Equations (2.2), (2.3), and (2.4), will obtain the cell parameter ( $a$ )

$$a = 2d_{100}/\sqrt{3} \quad (2.5)$$

A quantitative assessment of the porosity of mesoporous materials can be attempted on the basis of the only available parameters which seem to be independent of any assumption on the nature of the surface: the cell parameter ( $a$ ), the total pore volume ( $V_p$ ), and the mesopore diameter evaluated by the pressure of the mesopore-filling step of the isotherm ( $D_{BdB}$ ); hence, the mesopore diameter evaluated by the BdB method in equation 2.6.<sup>25</sup>

In the case of mesoporous materials, the geometrical model of a honeycomb structure formed by hexagonal pores accounts for all porosity parameters. From the geometrical model schematically depicted in Figure 2.5, the wall thickness ( $t$ ) can be evaluated as

$$t = a - 0.95D_{\text{BdB}} \quad (2.6)$$

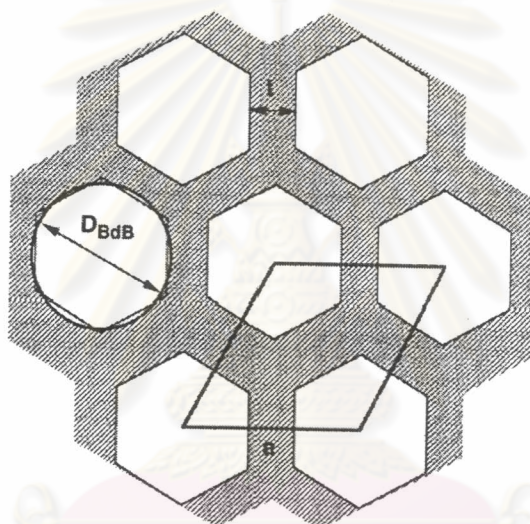


**Figure 2.5** A hexagonal cell showing the cell parameter ( $a$ ), the wall thickness ( $t$ ), and the cylindrical pore of  $D_{\text{BdB}}$  diameter which possesses the same section as the corresponding hexagonal pore<sup>26</sup>

### 2.1.3.2 Synthesis Strategies

The main general synthesis strategies used to construct these materials are shown in Figure 2.6. In all of these synthesis strategies, the chemical, spatial, and structural properties of the texturing agent, or the “reaction pockets”, must be thoroughly adjusted by controlling the rates of chemical reactions, the nature of the interfaces, and the

encapsulation of the growing inorganic phase.<sup>23</sup> An adequate tailoring of the organomineral interface is of utmost importance to obtain well-defined textured phases. The chemical, spatial, and temporal control of this “hybrid interface” is a major task in the challenge of developing cooperatively assembled inorganic-organic integrated systems. These synthesis strategies can be categorized following two principal approaches.

(a) The molecular/supramolecular templates are present in the synthesis media from the beginning; the self-assembly process of the templates is followed by (or synchronized with) the formation of the mineral network, deposited around the “self-assembled substrate”. Inorganic replication occurs at accessible interfaces built by preorganized or self assembled molecular or supramolecular templates, which create the mesostructure in the material. These templates can be organic compounds (surfactant molecules, amphiphilic block copolymers, dendrimers, etc.) or biomolecules, forming micellar assemblies or liquid crystal mesophases. They can also be preformed objects having submicronic, micronic, or macroscopic sizes, colloids (latex, silica), bacteria or virus, or even mesoporous silica frameworks that can be used as a template (nano- or microcasting) to embed any other component or material, being commonly used examples (route A). In many cases a cooperative self-assembly can take place in situ between the templates and the mineral network precursors yielding the organized architectures (route B).

(b) In the second approach, a nanometric inorganic component is formed (by inorganic polymerization or precipitation reactions). Nanoparticle formation can take place not only in solution but also in micelle interiors, emulsions, or vesicles, leading to complex shaped materials. The control of the dynamics of precipitation of this nanometric building block (NBB) is a key point when syntheses are performed under these conditions. These NBB can be subsequently assembled and linked by organic connectors or by taking advantage of organic functions dangling on the particle surface (route C).



The key feature in the synthesis of mesostructured materials is to achieve a well-defined segregation of organic (generally hydrophobic) and inorganic (hydrophilic) domains at the nanometric scale; here, the nature of the hybrid interface plays a fundamental role ( see in section 2.3).

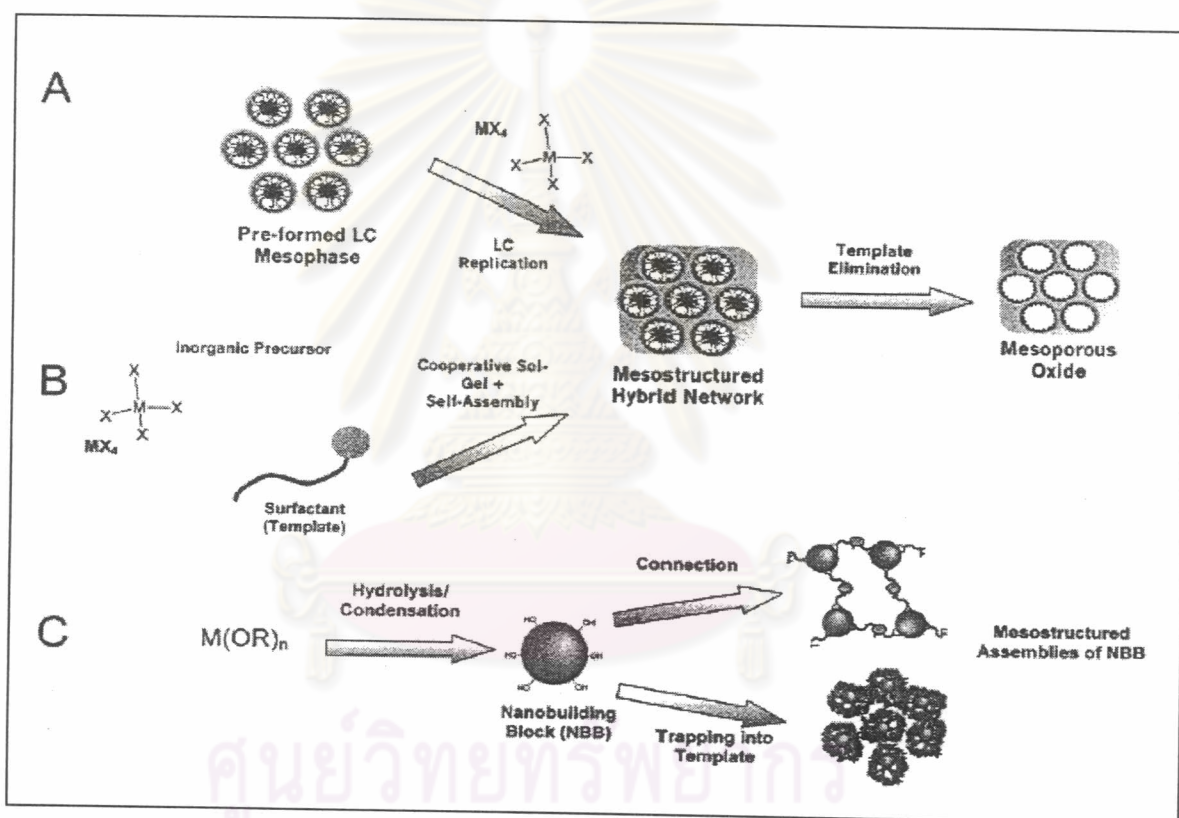
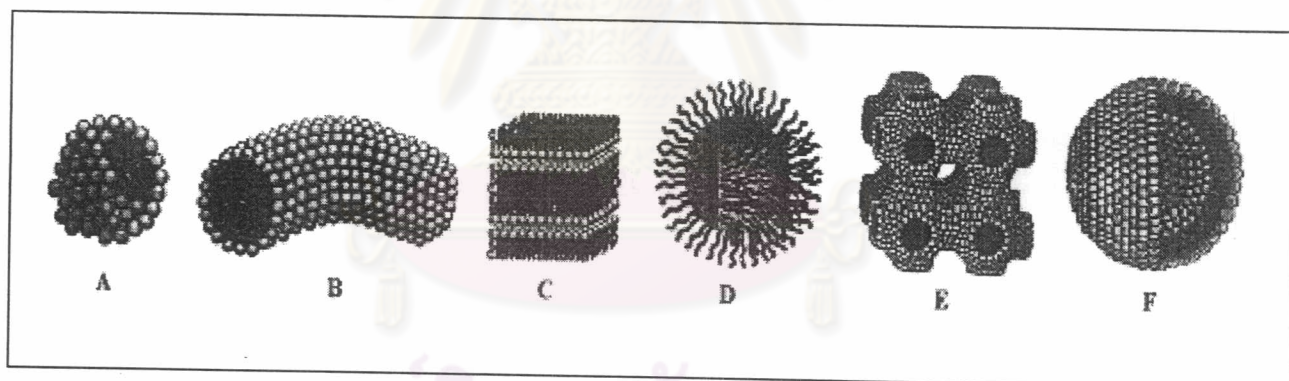


Figure 2.6 Main synthetic approaches for mesostructured materials<sup>23</sup>

Micellar aggregates organize according to different shapes (spherical or cylindrical micelles, lamellae) permitting the coexistence of two incompatible phases.<sup>27</sup> Some typical micellar structures are presented in Figure 2.7. In some colloidal systems, a more

complex behavior has been evidenced, and other arrangements, such as the spongelike bicontinuous structure (Figure 2.7E), are possible.

Upon progressive increase in surfactant concentration in the aqueous solution, a number of phases appear, always following the same order: direct spheres, direct cylinders, lamellae, inverse cylinders, and inverse spheres; this order corresponds to a monotonic variation of the interfacial curvature. Different models have been proposed to explain these experimental facts, the main parameters taken into account being (1) the hydrophobic interactions between organic chains, (2) geometric restrictions due to molecular packing, (3) molecule exchange between aggregates, (4) enthalpy and entropy of packing, and (5) electrostatic repulsion between polar heads.



**Figure 2.7** Micellar structures: (A) sphere (B) cylinder (C) planar bilayer (D) reverse micelles (E) bicontinuous phase (F) liposomes<sup>27</sup>

### 2.1.3.3 Role of the Polar Head Charge

Both surfactant and inorganic soluble species direct the synthesis of mesostructured MCM-41-type materials. The hybrid solids thus formed are strongly dependent on the interaction between surfactants and the inorganic precursors. In the case of

ionic surfactants, the formation of the mesostructured material is mainly governed by electrostatic interactions.<sup>27</sup> In the simplest case, the charges of the surfactant (S) and the inorganic species (I) are opposite, in the synthesis conditions. Two main direct synthesis routes have been identified:  $S^+I^-$  and  $S^-I^+$ . Two other synthesis paths, considered to be indirect, also yield hybrid mesophases from the self-assembly of inorganic and surfactant species bearing the same charge: counter ions get involved as charge compensating species. The  $S^+X^-I^+$  path takes place under acidic conditions, in the presence of halogenide anions ( $X^-$ ); the  $S^-M^+I^-$  route is characteristic of basic media, in the presence of alkaline cations ( $M^+$ ). The different possible hybrid inorganic/organic interfaces are shown in Figure 10. Table 4 gives different examples of mesostructured inorganic materials obtained following the above mentioned paths. Other synthesis routes rely on nonionic surfactants, where the main interactions between the template and the inorganic species are H-bonding or dipolar, giving birth to the so-called neutral path:  $S^0I^0$ ,  $N^0I^0$  and  $N^0FI^+$ .

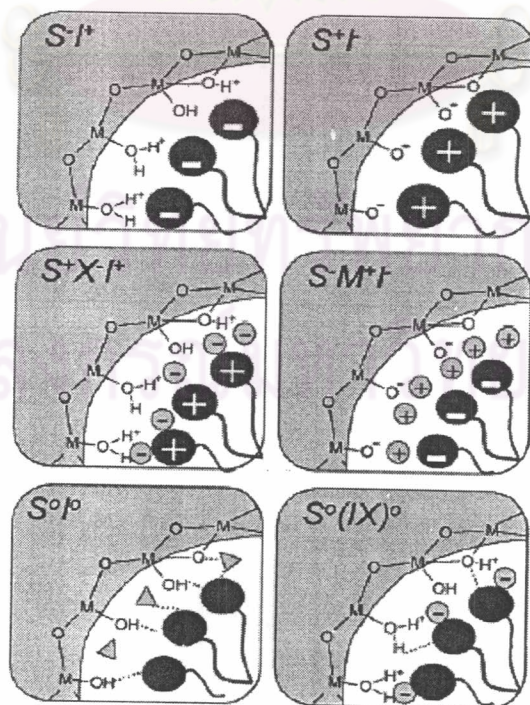


**Figure 2.8** Representation of the different types of silica-surfactant interfaces<sup>23</sup>

**Table 2.2** Examples of mesostructured inorganic materials with different interactions between the surfactant and the inorganic framework

Surfactant type	Interaction type	Example materials (structure)
cationic $S^+$	$S^+I^-$	silica: MCM-41 (hex) MCM-48 (cub) MCM-50 tungsten oxide (lam, hex) Sb oxide (V) (lam, hex, cub) tin sulfur (lam) aluminum phosphate (lam, hex)
	$S^+XI^+$	silica: SBA-1 (cub Pm3a) SBA-2 (hex 3D) SBA-3 (hex) zinc phosphate (lam) zirconium oxide (lam, hex) titanium dioxide (hex)
	$S^+FI^0$	silica (hex)
anionic $S^-$	$SI^+$	Mg, Al, Ga, Mn, Fe, Co, Ni, Zn (lam) oxides lead oxide (lam, hex) aluminum oxide (hex) tin oxide (hex) titanium oxide (hex)
	$SM^+I^-$	zinc oxide (lam) alumina (lam)
	$S^0I^0$	silica: HMS (hex)
neutral $S^0$ or $N^0$	$N^0I^0$	MSU-X (hex) silica (lam, cub, hex) Ti, Al, Zr, Sn (hex) oxides
	$N^0XI^+$	silica: SBA-15 (hex)
	$N^0FI^+$	silica (Hex)
	$(N^0M^{n+})IO$	silica (Hex)

(hex, hexagonal; lam, lamellar; cub, cubic)

## 2.2 Block Copolymer-Templated Mesoporous Materials

The first studying related to mesostructured oxides described the use of ionic surfactants such as the cationic alkyltrimethylammonium ( $C_nTA^+$ ,  $n = 8-18$ ), anionic alkylsulfonates ( $C_nSO_3^{2-}$ ,  $n = 12-18$ ) or alkylphosphates as supramolecular templates.<sup>28</sup> These synthesis were performed in extreme (acid or alkaline) pH conditions, yielding materials with controlled pore size (15-100 Å). However, two main limitations exist: (a) typical wall thickness of 8-13 Å, which is a serious limitations regarding stability for catalysis; (b) limited pore size offered by molecular surfactants. The only way to go beyond 50 Å pore size consisted in employing swelling agents, involving complicated synthesis, and irreproducibility (linked to emulsion formation or phase separation). Thus more versatile supramolecular templates were needed.

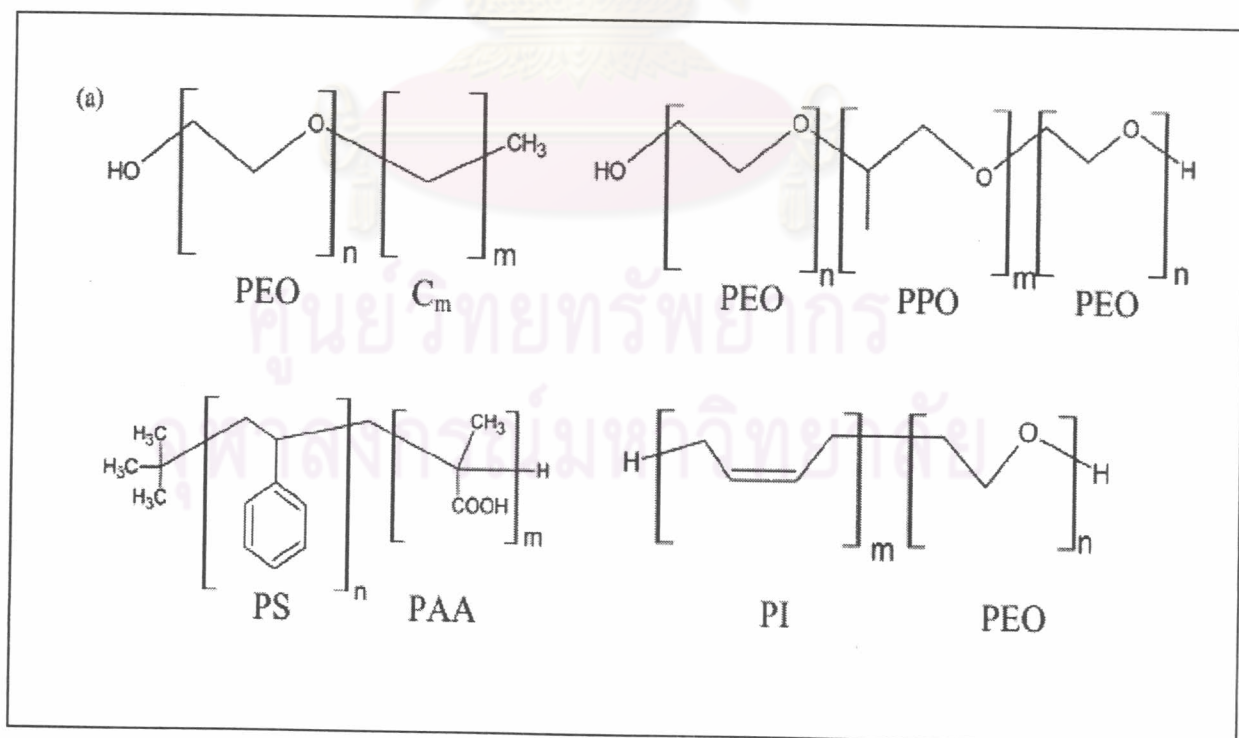


**Figure 2.9** Block copolymer used in mesostructure generation<sup>27</sup>

**Table 2.3** Characteristics of surfactants and block copolymer

<b>Surfactant</b>	<b>Block copolymer</b>
<i>Solution and mesophase behavior</i>	
Molecular/monodisperse	Polymer can be polydisperse
Head+chain structure object shape controlled by the $g$ packing parameter	Enormous range of architectures: linear, branched, star and shape
Simple micelle-like or bi-continuous mesostructures	Possibility of complex multiscale mesostructures (e.g. 'knitting patterns')
Micellization driven by Hydrophilicity/hydrophobic character	Micellization driven by Hydrophilic/hydrophobic character, block size and conformation
Cosolvent swelling modifies curvature by cosolvents	Differential swelling of domains
<i>Use in the design of mesostructured materials</i>	
'Hard' well-defined HI	'Blurry' interface, swollen by the inorganic phase
Thin walls (1–1.5 nm)	Thick walls (2–10 nm)
Walls not entangled with the template	Walls entangled with the template ('multiphase')
Pore size limited by micelle size	Pore size tailorable by modifying the polymerization degree, monomer nature or polymer fraction

Amphiphilic block copolymer belongs to an important family of surfactants, widely used in detergency, emulsifying, coating, thickening, etc. The self-assembly characteristics of these block copolymer permit to control the superstructure, to vary the typical length scales and to add specific functions. Indeed, the properties of block copolymer can be continuously tuned by adjusting solvent composition, molecular weight or polymer architecture. Figure 2.9 shows typical block copolymer used as templates and Table 2.3 compares the characteristics of block copolymer vs. low-weight ionic surfactants. In term of block copolymer-template can be classified following three methods.

Oligomeric nonionic surfactants, alkyl poly(oxyethylene) and poly(oxyalkylene), have been widely used and compared to true block copolymer templates<sup>29</sup> (although not strictly block copolymer). Hereafter, these kinds of polymers are described.

#### (a) Precipitation-based method

Pinnavaia and coworker<sup>20</sup> were the first to bring the idea of using nonionic surfactants (alkylamines ( $C_nNH_2$ ), oligomeric alkyl-poly(ethylene oxide) ( $C_n(PEO)_mOH$ ), or  $(PEO)_m(PPO)_n(PEO)_m$ ,  $EO = -CH_2CH_2O-$ , and  $PO = -CH(CH_3)CH_2O-$ ) as porogen species, in neutral media. Some advantages of using neutral non-ionic surfactants over the ionic ones were immediately noticed: (a) larger inorganic wall thickness (15-40 Å), enhancing the hydrothermal stability of the mesoporous oxides; (b) easier pore diameter tuning, by varying both the type and the concentration of the surfactant, (c) easier solvent removal, by solvent extraction: H-bonding (instead of electrostatic) interactions between the template and the inorganic framework should be easier to dissociate.

### (b) True Liquid Crystal Templating

Silica sol-gel was polymerized in lyotropic liquid crystals (LC), creating an alternative to conventional precipitation methods (the true liquid crystal templating, TLCT route). This path leads to mesostructured hexagonal, cubic or lamellar silica, as gels, cast monoliths or membranes. Metallic mesoporous materials are obtained by chemical or electrochemical reduction of metal salts, dissolved in the hydrophilic regions of the LC phase. A similar approach leads to ordered arrays of semiconductor nanoparticles.

TLCT methods give a cast replica of the LC phase; the final phase should be in principle controlled by knowing the phase diagram of the surfactant (a kind of thermodynamic control). However, a major drawback is the inhomogeneity that can result either by inadequate diffusion of the inorganic moieties within the pre-formed LC phase, or uncontrolled phase. Separation due to inorganic polymerization taking place in viscous LC media. While PEO-PPO-PEO or PEO-alkyl copolymers are the most usual templates, Antonietti and coworkers extended the TLCT approach to a great variety of inorganic frameworks and polymeric templates, particularly to high molecular mass ionic copolymers or poly(ethylene-co-butylene)-*b*-(ethylene oxide), which afford very large pore size (20–30 nm). This group has also used PS-PEO BC, which lead to quasi-hexagonal pore arrangements.

### (c) Evaporation-Induced Self Assembly

The evaporation-induced self assembly (EISA) denomination was coined to encompass the synthesis methods leading to ordered hybrid mesophases from dilute solutions, upon solvent evaporation. EISA can be considered an LCT-based method (after solvent



evaporation, a hybrid LC phase is formed). Starting from solutions below the critical micellar concentration, permits one to obtain thin films or gels with excellent homogeneity (high dilution discouraging inorganic polymerization). BC-templated silica mesoporous films and monoliths were obtained by EISA. This method is particularly interesting to work with non-silica systems, where condensation has to be thoroughly controlled.

### 2.2.1 Formation of Mesostructure with Block Copolymer

Two main processes can be recognized in the formation of these mesophases, with block copolymer<sup>30</sup> which is schematized in Figure 2.10.

a) The creation of an organized texture, due to the self-assembly properties of the template. This process results in a microphase separation, which divides the space in two domains : hydrophilic and hydrophobic, in the case of the simplest block copolymer surfactants.

b) The formation of an inorganic network. The inorganic components are placed in one of the spatially separated parts of these nanoheterogeneous systems. Condensation reactions will give rise to an extended inorganic network; these reactions can be tuned to take place simultaneously or subsequently as organization proceeds.

The simplest analysis will evidence three fundamental interactions that will control the final obtained structure: surfactant-surfactant (S-S), inorganic-inorganic (I-I) and surfactant-inorganic (S-I); these interactions take place in each of the microsegregated phases, or at the inorganic-template hybrid interface (HI). The solvent will also take part in mesophase formation. The most relevant thermodynamic aspects in the formation of a hybrid

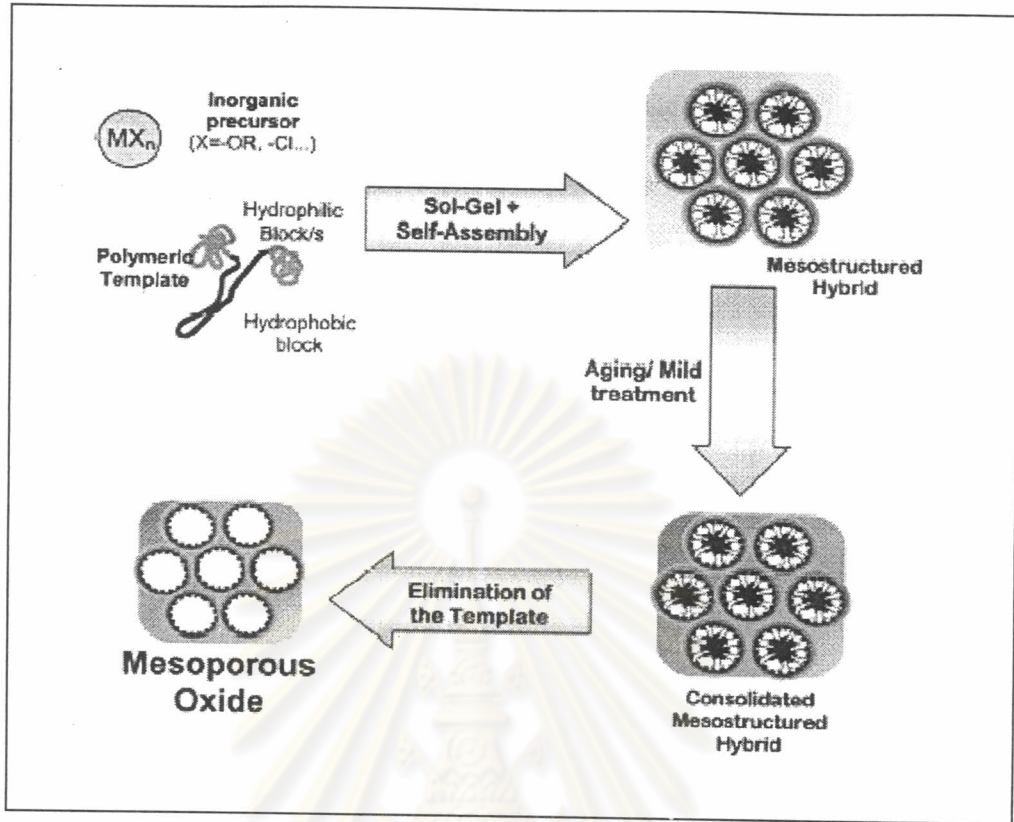


**Figure 2.10** The steps leading from a solution to a mesoporous oxide network<sup>27</sup>

mesophase ( $\Delta G_{ms}$ ) have been defined in their description of the cooperative assembly model.

$$\Delta G_{ms} = \Delta G_{inter} + \Delta G_{inorg} + \Delta G_{org} + \Delta G_{sol}$$

The central points to a well-defined mesophase formation<sup>31</sup> are (a) the adequate segregation of hydrophilic and hydrophobic regions of the template (mainly  $\Delta G$ ) (b) the selective positioning of the inorganic counterpart in one of these regions, without disrupting organization; this is related to the creation of a well-defined and compatible HI between the inorganic walls and the organic templates (i.e.  $\Delta G_{org}$  is important). In principle,  $|\Delta G_{inorg}| < |\Delta G_{inter}|$  or  $|\Delta G_{org}|$  to permit the latter two terms to direct the formation of organized assemblies. Obtaining a well-defined templated hybrid is a matter of controlling a delicate

thermodynamic and kinetic balance between multiple phenomena. Figure 2.11 shows the three main components of a mesostructured hybrid (template, inorganic and solvent), connected by their binary relationships. This gives a first-order general picture of the important variables.

An important advantage of block copolymer compared to ordinary surfactants is that all relevant terms leading to order (i.e.  $\Delta G_{\text{inter}}$  and  $\Delta G_{\text{org}}$ ) can be pre-designed from the synthesis. The hydrophilic/lipophilic balance (HLB) and shape can be tuned by changing the polymerization degree. Moreover, the intrinsic chemistry of each block can be changed, modulating the interactions with the inorganic units that build up the framework.

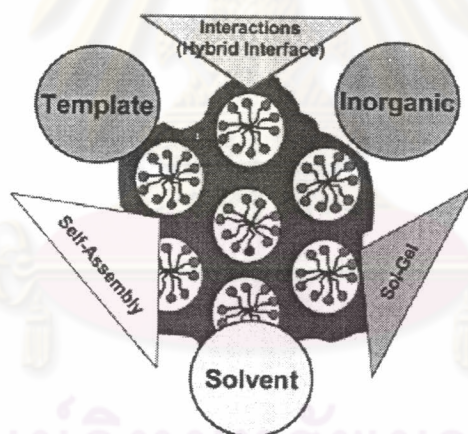


**Figure 2.11** The main relationships between the solvent, the template and the inorganic center<sup>31</sup>

### 2.2.3 The Role of the Hybrid Interface

The S-I interaction is particularly important in block copolymer-metal oxide hybrids, especially in PEO-PPO based ones. Different possible interactions taking place at the HI are shown in Figure 2.12. Schematic view of the  $(S^0 H^+)(X^- I^-)$ ,  $S^0 I^0$ , and  $(S^0 M^+)(X^- I^-)$

HIs and three possible structures of a HI composed by a nonionic polymer and an inorganic framework are shown in Figure 2.12. Right, a three-phase HI, the PEO block is completely segregated from the inorganic phase. Center, an intermediate situation, where a fraction of the PEO is free. Left, a two-phase HI where the inorganic polymer is completely integrated into the PEO block. Most of the fine HI characterization has been performed on PEO-based (di- or triblock) templates.

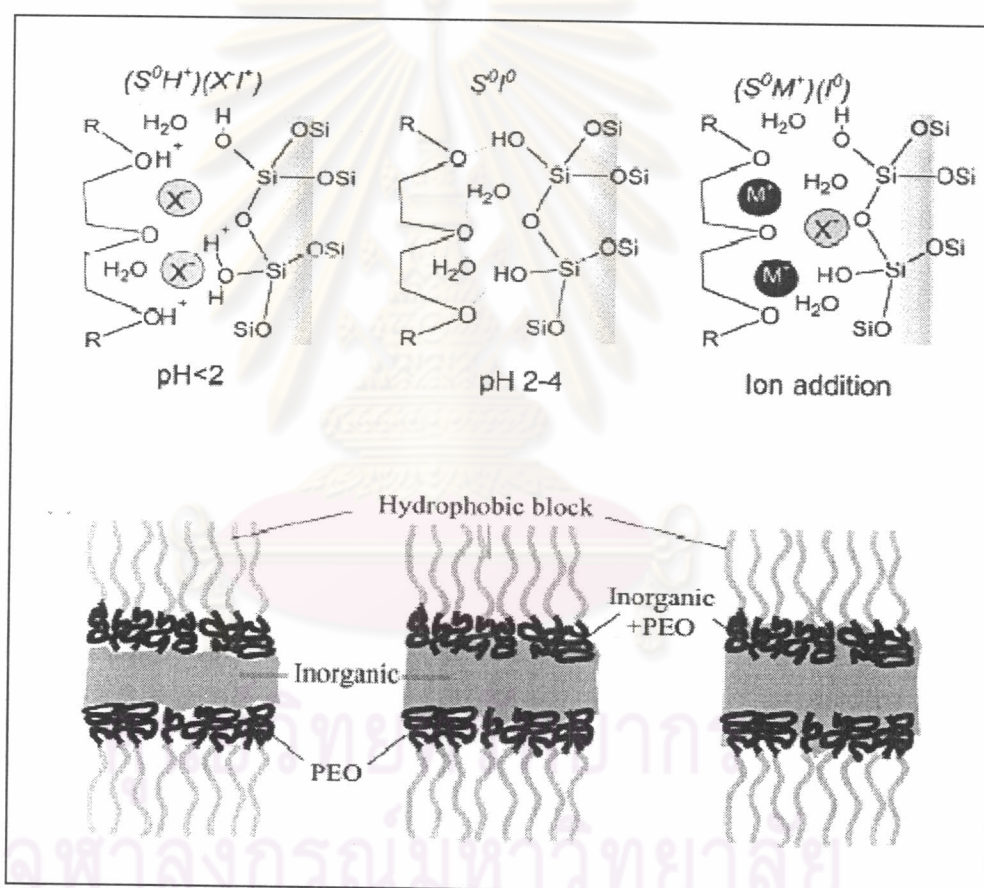


Figure 2.12 Different possible interactions of a HI<sup>27</sup>

Melosh *et al.*<sup>32</sup> determined that in F127-templated silica monoliths, organization arose for polymer weight fractions higher than 40%. For lower polymer/silica ratios, non-ordered gels were formed. This lack of order was due to a relatively strong

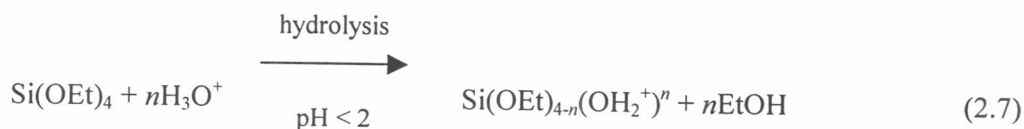
interaction (probably of H-bonding type) of the (Si-O-Si) polymers forming the inorganic skeleton with both PEO and PPO blocks. These strong interactions extend the HI, hindering PPO segregation. For higher polymer concentrations, the PPO/PPO (S-S) attractions take over the Si-O/PPO (S-I) interactions, and microsegregation takes place, resulting in mesostructural order. In all examined cases, a strong interaction was observed between the PEO block and the silica polymer. A similar feature has been proposed to explain the porosity of SBA-15.

## 2.3 SBA-15

### 2.3.1 Porosity of SBA-15: Formation Mechanisms

The formation of an organized hybrid mesostructure is the result of the balance between two competitive processes: phase separation/organization of the template vs. inorganic polymerization.

On the basis of these results able to be postulated that the assembly of the mesoporous silica SBA-15 organized by poly(alkylene oxide) triblock copolymer species, PEO-PPO-PEO in acid media occurs through an (S<sup>0</sup>H<sup>+</sup>)(X-I<sup>+</sup>) pathway. First, alkoxy silane species (silica source) are hydrolyzed which is followed by partial oligomerization at the silica as shown in equations 2.7 and 2.8.<sup>29</sup>



The EO moieties of the surfactant in strong acid media associating with hydronium ions



where R = poly(propylene oxide) and  $\text{X}^- = \text{Cl}^-$ . These charge-associated EO units and the cationic silica species are assembled together by a combination of electrostatic, hydrogen bonding, and van der Waals interactions  $\text{REO}_{m-y}[(\text{EO})\cdot\text{H}_3\text{O}^+]_y \cdots y\text{X}^- \cdots \text{I}^+$ , which can be designated as  $(\text{S}^0\text{H}^+)(\text{X}\text{T}^+)$ . Coordination sphere expansion around the silicon atom by anion ( $\text{Cl}^-$ ) coordination of the form  $\text{X}^- \cdot \text{Si}-\text{OH}_2^+$  may play an important role. During the hydrolysis and condensation of the silica species, intermediate mesophases, as hexagonal for SBA-15.

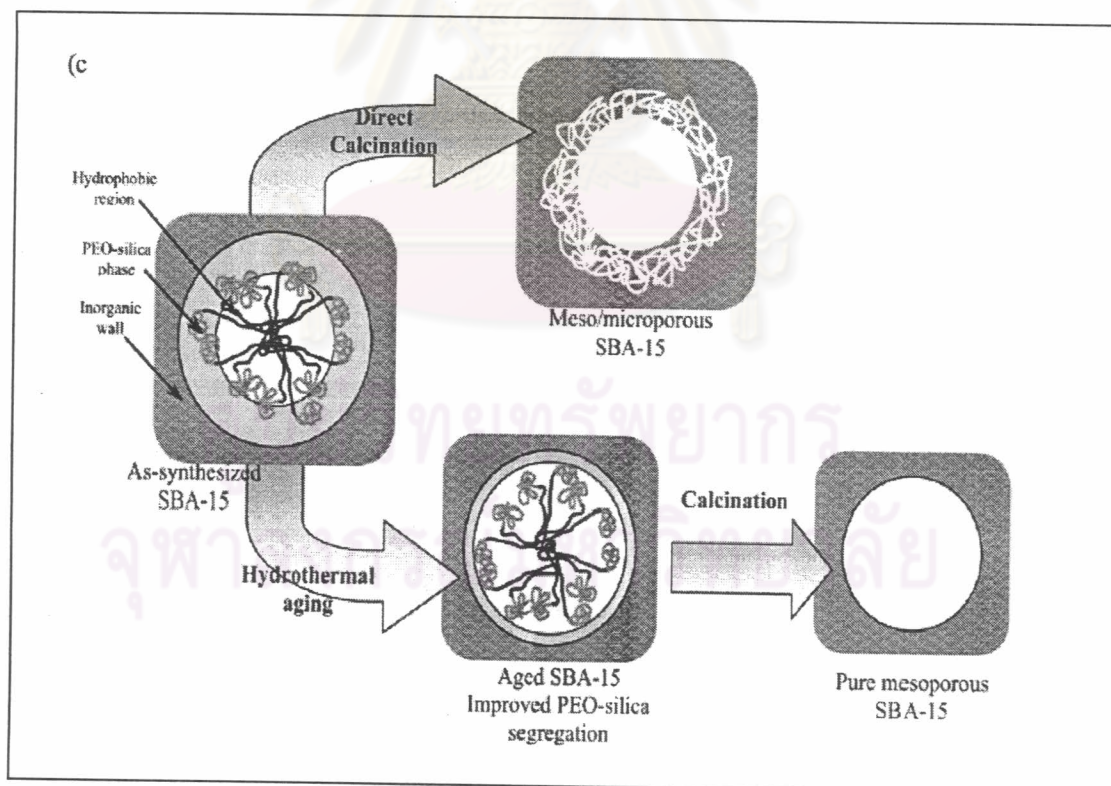


**Figure 2.13** Scheme of the pore evolution upon thermal treatment, depending on pre-treatment and aging<sup>27</sup>

For SBA-15 materials, aging time and temperature are particularly important.<sup>33</sup>

It found that mesoporous SBA-15 prepared from calcinations of an 'as-prepared' hybrid precursor contained a significant fraction of microporosity; further aging of the precursor in the mother liquors leads to an improvement on the pore size distribution as shown in Figure 2.13.

### 2.3.2 The Features of SBA-15

Hexagonal mesoporous silica structures, SBA-15, with tunable large uniform pore sizes (up to  $\sim 300$  Å) are obtained by use of amphiphilic block copolymers as organic structure-directing agents. Using aqueous acidic conditions and dilute triblock copolymer concentration, SBA-15 has been synthesized with a highly order two-dimensional hexagonal mesostructure and thick uniform silica walls. The thick silica walls, in particular, are different from thinner walled MCM-41 structures made with conventional cationic surfactants and lead to greater hydrothermal stability on the part of SBA-15.

SEM images reveal that as-synthesized SBA-15 has a wheatlike macroscopic particle morphology with uniform mean sizes of about  $80 \mu\text{m}$  and these consist of many ropelike<sup>34</sup> aggregates as shown in Figure 2.14. Calcined SBA-15 shows a similar particle morphology, reflecting the thermal stability of the macroscopic structure.

For SBA-15 materials, aging time and temperature are particularly important.<sup>5</sup> Heating as-synthesized SBA-15 in the reaction solution at different temperatures ( $80$ - $140$  °C) and for different lengths of time ( $11$ - $72$  h) results in a systematic series of structures as illustrated in Table 2.4 with different pore sizes ( $47$ - $89$  Å) and different silica wall thicknesses ( $31$ - $64$  Å). Higher temperatures or longer reaction times result in larger pore sizes and thinner silica walls. The large pore sizes and silica wall thicknesses may be caused by the relatively

(31-64 Å). Higher temperatures or longer reaction times result in larger pore sizes and thinner silica walls. The large pore sizes and silica wall thicknesses may be caused by the relatively long hydrophilic EO blocks of the copolymer. Increasing the temperature results in increased hydrophobicity of the EO block moiety and therefore decreases, on average, the lengths of the EO segments that are associated with the silica wall as illustrated in Table 2.4. This tends to increase the hydrophobic volumes of the surfactant aggregates, resulting in the increased pore sizes in SBA-15 materials prepared at higher temperatures (80 °C).

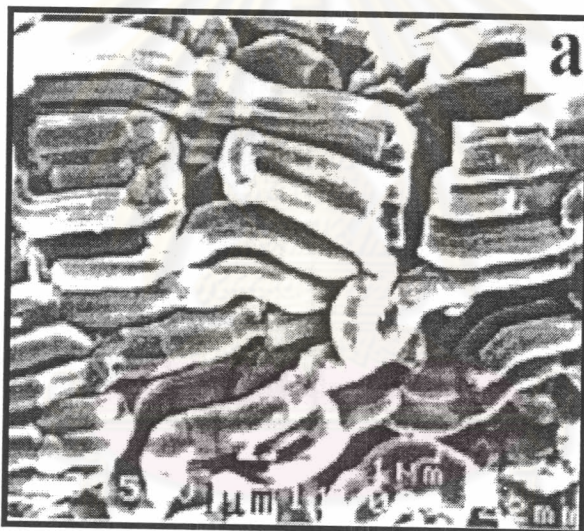


**Figure 2.14** SEM image show morphology of SBA-15<sup>5</sup>

**Table 2.4** Physicochemical properties of SBA-15 with various aging time and temperature

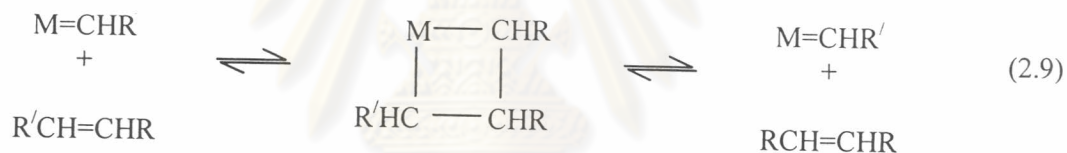
Aging conditions (° C)	$d$ (Å)	BET surface area (m <sup>2</sup> /g)	Pore size (Å)	Pore volume (cm <sup>3</sup> /g)	Wall thickness (Å)
35 ° C, 20h	104 (95.7)	690	47	0.56	64
80 ° C, 24h	105 (97.5)	780	60	0.80	53
80 ° C, 48h	103 (99.5)	820	77	1.03	38
90 ° C, 24h	108 (105)	920	85	1.23	36
100 ° C, 24h	105 (104)	850	89	1.17	31



## 2.4 Olefin Metathesis

### 2.4.1 Definition of Olefin Metathesis

Olefin metathesis is the olefin disproportionation reaction<sup>7</sup> in which is one of the most original and unusual transformations in chemistry as shown in equation 2.9. In this reaction, alkene are converted into new products via the rupture and reformation of carbon-carbon double bonds. Remarkably, the strongest bond in the alkene, the C=C double bond, is broken during the reaction. The resulting RHC= fragments are exchanged between the alkenes that participate in the reaction.



In the presence of certain transition-metal compounds, including various metal carbenes, olefins exchange the groups around the double bonds, resulting in several outcomes: straight swapping of groups between two acyclic olefins (cross-metathesis), closure of large rings (ring-closing metathesis), formation of dienes from cyclic and acyclic olefins (ring-opening metathesis), polymerization of cyclic olefins (ring-opening metathesis polymerization), and polymerization of acyclic dienes (acyclic diene metathesis polymerization). And different types of monoolefin and diolefin undergo metathesis via contact with a suitable catalyst, resulting in a wide variety of possible products as shown in equations 2.10-2.12.<sup>2</sup>

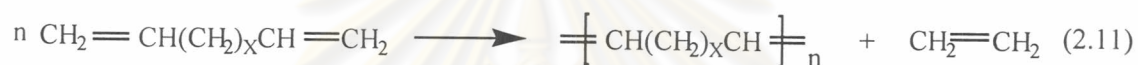
## Acyclic olefins




(R and R' = alkyl or H)

## Diolefins

## Intermolecular Reaction



## Intramolecular Reaction

(where  represents a hydrocarbon chain with or without a heteroatom)

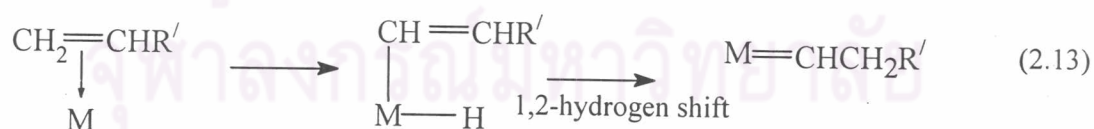
All the reactions are reversible, and when volatile or soluble products are formed, displacement of the equilibrium occurs. Thus when R = H, removal of ethylene from the system of equation can drive the reaction to completion. The reverse reaction is called cross-metathesis and cross metathesis with ethylene is called ethanolysis. Both linear and branched olefins can undergo metathesis.

Diolefins, such as  $\alpha,\omega$ -dienes, undergo intermolecular and intramolecular metathesis. Intermolecular reactions, as shown in Equation 2.12, eventually lead the production of high polymers, known as acyclic diene metathesis (ADMET) polymers. If the

diolefin couples undergo intramolecular to produce a cyclic alkene, the process is called ring-closing metathesis (RCM). The reverse reaction is called ring opening cross-metathesis. In general, ADMET is favored in highly concentrated solutions or when the substrate is neat, whereas RCM is favored at low concentrations. The relative occurrence of ADMET and RCM also depends on the size of the ring formed.

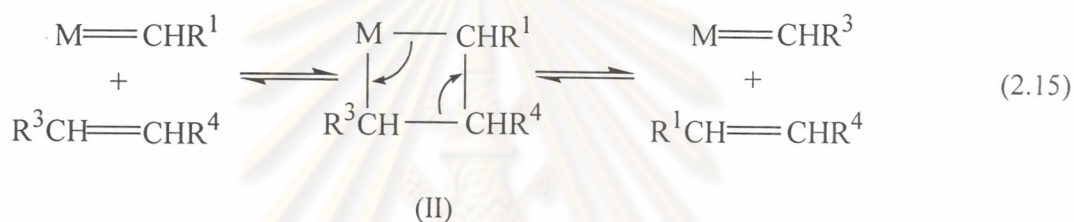
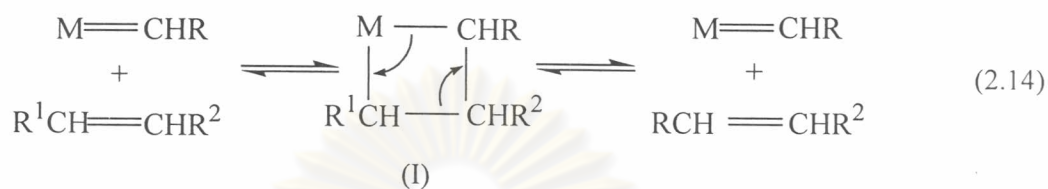
#### 2.4.2 Mechanism of Olefin Metathesis

The fundamental step in olefin metathesis is exchanging between a metal carbene and an olefin. Mechanism of olefin metathesis concerns a transalkylidene reaction and it is generally accepted that the reaction proceeds via the so-called metal carbene mechanism. In the heterogeneous metathesis, the initial metal carbene can be formed by interaction of the substrate alkene with the transition metal center.<sup>7</sup> The most accepted route to the first metal carbene is the formation of a  $\pi$ -complex between the reacting alkene and the transition metal, followed by either a 1,2-hydrogen shift mechanism as shown in equation 2.13.



The propagation reaction involves a transition-metal carbene as the active species with a vacant co-ordination site at the transition metal. The alkene co-ordinates at this

vacant site, and subsequently a metallacycle is unstable and cleaves to form a new metal carbene complex and a new alkene as shown in equations 2.14 and 2.15.



If metallacyclobutane intermediates formed by reacting olefin with the metal-alkyldene complex on heterogeneous catalyst, metal-alkyldene sites  $[\text{M}=\text{CHR}]$  should be firstly formed on the surface from adsorbed olefins. It able to be demonstrated by using  $\text{MoO}_3$  film sublimated on a quartz tube. Once metal-alkyldene sites are formed on the surface, the olefin metathesis reaction is catalyzed on the sites as described in Figure 2.15 until the alkyldene species are dismissed by some side reactions, which is analogous to the olefin isomerization reaction. Therefore, this can say that the olefin metathesis catalysts developed so far are the materials on which  $[\text{M}=\text{CHR}]$  sites are formed automatically from adsorbed olefins.

The metathesis reaction of alkene involves two types of the metathesis reaction as described by equation 2.16 for reaction of propylene. So far, however, productive metathesis (i) has been mainly studied because the degenerate metathesis of propylene (ii) can be recognized by using isotope labeled olefins. As we can use deuterium labeled olefins on

our activated catalyst, degenerate or cross-metathesis of propylene (ii) can be detected. Therefore, it would be possible to derive a total mechanism for the productive and degenerate metathesis reaction of propylene.

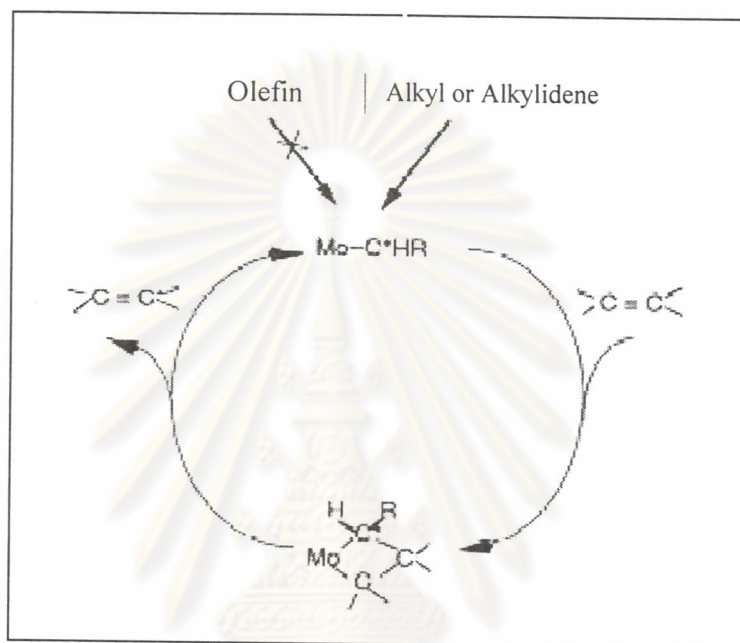


**Figure 2.15** The olefin metathesis reaction is catalyzed on the metal–alkylidene sites which are formed by the adsorption of olefins or by some other reactions<sup>34</sup>

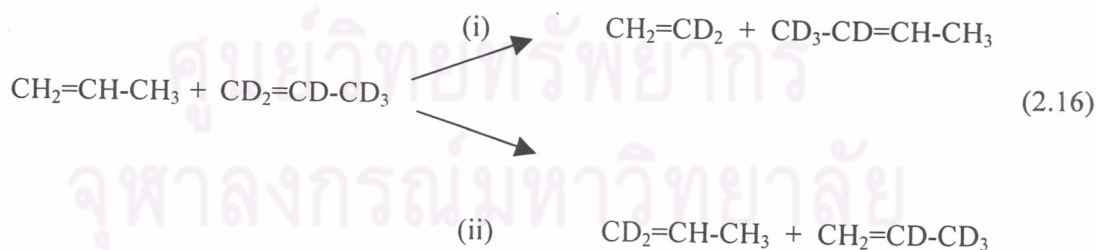


Figure 2.16 shows a total mechanism for the propylene metathesis reaction, where the productive metathesis is brought about by alternative formation of  $\text{Mo}=\text{CH}_2$  and

$\text{Mo}=\text{CH}-\text{CH}_3$  sites and the degenerate metathesis reaction occurs on either  $\text{Mo}=\text{CH}_2$  or  $\text{Mo}=\text{CH}-\text{CH}$  sites by reproducing the same alkyldene sites. It is interesting to note that either site of  $\text{Mo}=\text{CH}_2$  or  $\text{Mo}=\text{CH}-\text{CH}_3$  predominantly contributes to the degenerate metathesis of propylene.

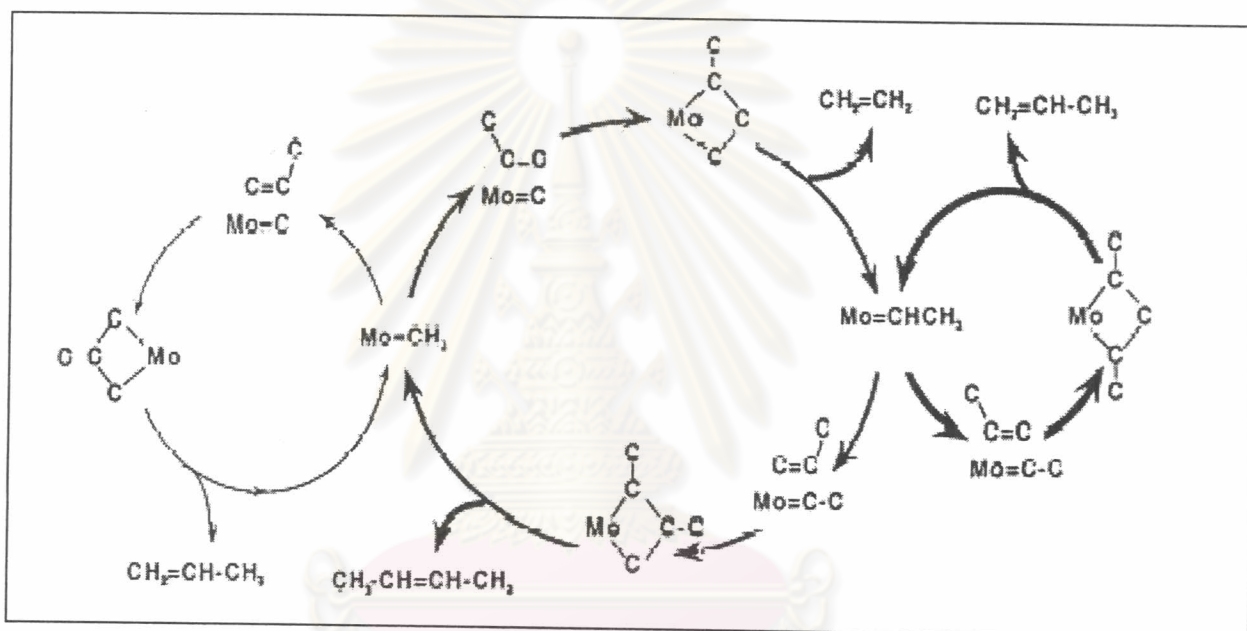


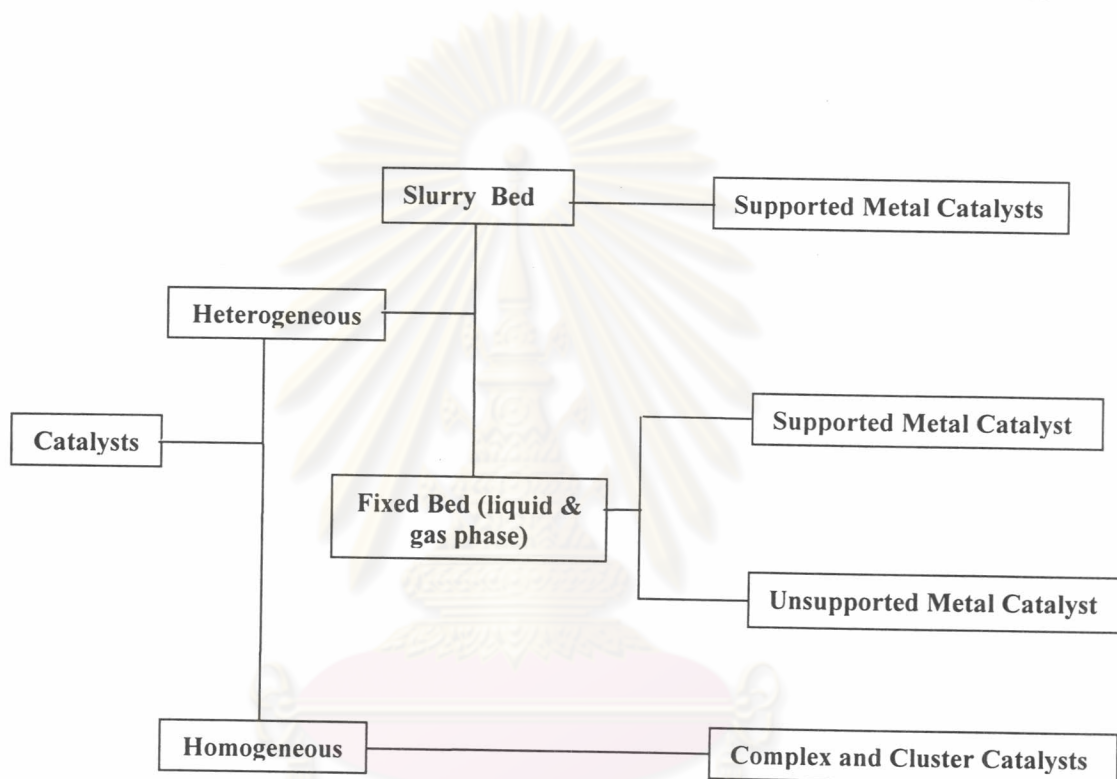
Figure 2.16 Total mechanism for the propylene metathesis reaction<sup>34</sup>

## 2.5 Olefin Metathesis Catalysts

### 2.5.1 Supported Metal Catalysts

Supported metal catalysts are in the group of heterogeneous catalyst<sup>13</sup> as shown in scheme 2.1. The supported metal catalysts generally have strong tendency for the chemisorption of hydrogen, oxygen, carbon monoxide and light hydrocarbons. Thus they are

often used in several reaction involving hydrocarbons. The catalyst is generally composed of one or two transition metals, particularly the noble metals, and a stable porous support with high surface area of support and metal. The reaction with this type of catalyst is often very sensitive to the metal crystalline structure and active site distribution on surface of support.



**Scheme 2.1** Classification of catalysts

The oxides of rhenium, molybdenum and tungsten deposited on a high surface area support (an inorganic oxide) are among the more effective heterogeneous catalysts for olefin metathesis. The structures and properties of supported metal oxide species are often strongly influenced by various factors such as support, promotor. Hereafter, the most three types active metal for metathesis are described.

### (a) Rhenium

Rhenium oxide on alumina is the most common catalyst in this class. The metal is softer, in spite of the high oxidation state, and reaction conditions are less harsh. Several studies supported rhenium oxide catalysts for olefin metathesis. The structure of alumina-supported rhenium oxide after calcination is described by Mol and coworker.<sup>7</sup> Mainly monomeric tetrahedrally coordinated  $\text{ReO}_4^-$  ions are present, besides minor amounts of species with Re-O-Re bonds; the concentration of the latter increases with the rhenium loading. For simple alkenes at all loadings the system exhibits catalytic activity, but the turnover frequencies dramatically increase with the rhenium loading.

In contrast to what has been observed for the  $\text{Re}_2\text{O}_7/\text{Al}_2\text{O}_3$  catalyst, the specific catalytic activity (turnover frequency) decreases with increasing rhenium content when  $\text{SiO}_2\text{-Al}_2\text{O}_3$  is used as the support. A high activity is obtained for a silica-alumina-supported catalyst with an alumina content of about 25 wt% alumina, which has the highest Brønsted acidity. This Brønsted acidity is due to two types of hydroxyl groups: hydroxyl groups attached to a Si atom and bridging hydroxyl groups attached to both Si and an Al atom. The latter type of hydroxyl groups is more electron-poor more Brønsted acidic than the silanol groups. At low rhenium loadings,  $\text{ReO}_4^-$  ions react preferably with the Si-Al bridging surface hydroxyl groups during calcination, resulting in electron-poor rhenium centers ( $\text{ReO}_4$  tetrahedra), the active site precursors. This might explain why  $\text{Re}_2\text{O}_7$  supported on silica-alumina is very active at low rhenium loadings. At higher rhenium loadings the hydroxyl groups attached to a Si atom are also replaced, resulting in inactive rhenium centers of the type  $\equiv\text{Si-O-ReO}_3$  (or rhenium clusters), as it is known that  $\text{Re}_2\text{O}_7/\text{SiO}_2$  has no activity in olefin metathesis. The inactivity of  $\text{Re}_2\text{O}_7/\text{SiO}_2$  might be due to the fact that  $\text{SiO}_2$  does not stabilise the necessary intermediate oxidation state of rhenium. From studying of this



behaviour, there is an apparent discrepancy in the hypothesis that the  $\text{ReO}_4^-$  ions react first with the acidic hydroxyl groups of the silica-alumina support, but with the Lewis acid and subsequently the basic hydroxyl groups of the alumina support. In fact, the role  $\text{ReO}_4^-$  species prefer to bind to aluminium containing sites, either during impregnation or during calcination.

### (b) Molybdenum

The ubiquitous molybdenum-containing catalysts is molybdenum oxide supported on a solid matrix of alumina, silica or related materials.<sup>3</sup> It is well known that molybdenum oxides are active for many reactions, including metathesis, concurrently the first discovery of metathesis reaction. The catalytic performance of molybdenum oxide from different precursors and different processing parameters are consecutively studied. To improve the activity of  $\text{MoO}_3/\text{Al}_2\text{O}_3$  catalyst for olefin metathesis also involves the addition of a third component. Incorporating  $\text{Re}_2\text{O}_7$  into  $\text{MoO}_3/\text{Al}_2\text{O}_3$  can increase the activity for metathesis of 1-hexene, but the product distribution is almost the same found for  $\text{MoO}_3/\text{Al}_2\text{O}_3$ .<sup>35</sup> It seems that the Re cation is capable of creating efficient metathesis sites, but the rate of metathesis is still not large enough to compete with the rate of isomerization. Due to the active sites arising from Mo-Al surface species are mainly responsible for the isomerization of 1-hexene, while the active sites which are responsible for metathesis of hexane are mostly represented by surface Re species. The reaction scheme of the metathesis of 1-hexene over the catalyst can be expressed as follows in Figure 2.18.

In addition, a recent study pointed out the oxidation state of molybdenum active species for metathesis of propylene. The formation of  $\text{Mo}^{4+}$  monooxo active species on  $\text{MoO}_3/\text{SiO}_2$  were formed by prereduction with CO under photoirradiation<sup>3</sup> while  $\text{Mo}^{4+}$  monooxo species on  $\text{MoO}_3/\text{Al}_2\text{O}_3$  were generated by  $\text{H}_2$  prereduction, resulting active

metathesis catalyst. Whereas some reports showed that  $\text{Mo}^{5+}$  dioxo-species on  $\text{SiO}_2$ , which produced by photo-reduction with CO is also effective for metathesis.

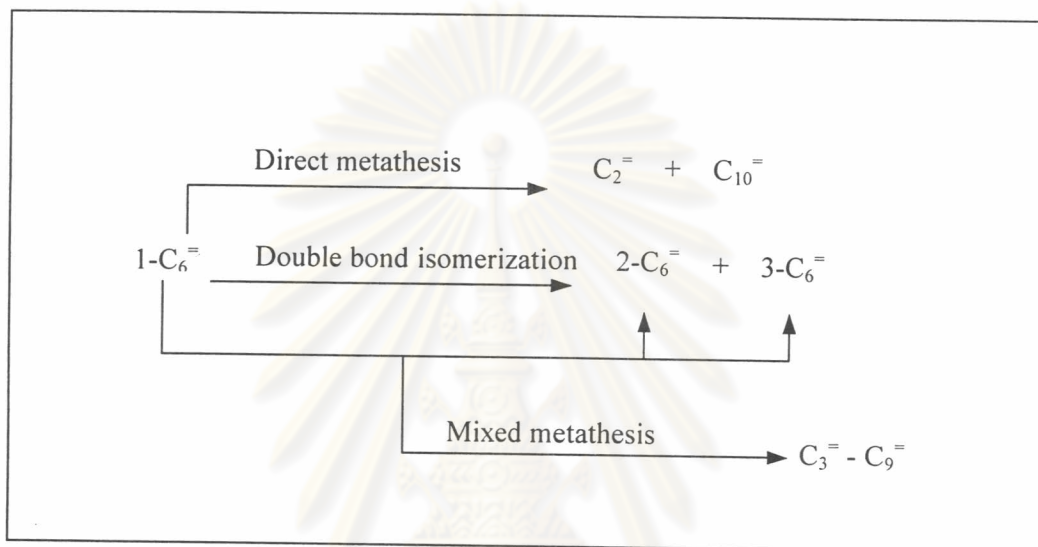


**Figure 2.17** Metathesis of 1-hexene in the presence of isomerization<sup>35</sup>

**(c) Tungsten**

Tungsten catalysts are essentially variation of molybdenum analogues. It has been widely accepted that analogous metal carbene species are formed on the surface of heterogeneous metathesis catalyst.<sup>3</sup> Using tungsten to prepare metathesis catalysts were accepted by many researchers. Conventionally, silica-supported tungsten oxide ( $\text{WO}_3/\text{SiO}_2$ ) is the one of the most widely used heterogeneous catalysts in the metathesis of olefin.<sup>36</sup> Although supported tungsten oxide catalysts are less active for metathesis than their rhenium and molybdenum counterparts, These catalysts have been reported to have considerable resistance to poisons as might be expected from the high operating temperature.<sup>37</sup> The online

lifetime of catalytic system with tungsten catalysts is also greater than both the rhenium and molybdenum systems and it can also be regenerated continuously without any adverse effect on structure and activity.<sup>37</sup> However, tungsten oxide on other supports in metathesis were studied. Alumina-supported tungsten were studied in propylene metathesis. This catalyst is active in side reactions such as polymerization, isomerization and cracking. Studies showed the Brønsted acid sites generated on catalyst to be responsible for the lateral acid-catalyzed reactions. It indicated that tungsten oxide on alumina is not good catalysts for metathesis.

In industry,  $\text{WO}_3/\text{SiO}_2$  has used as metathesis catalyst in a fixed bed reactor of OCT (Olefin Conversion Technology) process for propylene production and cross-metathesis for neohexene production.

## 2.5.2 Catalyst Preparation

### 2.5.2.1 Impregnation

Impregnation of support materials with a catalytically active phase is frequently employed when small percentages of active material are required. This technique is centered around the aqueous deposition of an active precursor on a support.

#### (a) Wet Impregnation

Wet impregnation occurs when an excess of aqueous material is added to the support medium. The volume of aqueous precursor is equal to or less than the pore column of the support. This technique facilitates active metal deposition for systems with weak or no support/metal interaction. By varying the solution properties (concentration,

temperature, pH and ionic strength) one can control the final supported catalyst attributes (particle size, dispersion and amount).

**(b) Dry or Incipient Wetness Impregnation**

The metal loading in the finished catalyst that prepared by this method is typically small amount. This method allows accurate control of the amount of the active ingredient that will be deposited into the catalyst. The porous support is contacted, as by spraying, with a solution of metal salt with appropriate concentration. Incipient wetness is the situation when the pores have been filled but the outside of the grain is dry. The impregnated support are then dried and calcined to transform the metal to active form.



ศูนย์วิทยทรัพยากร  
จุฬาลงกรณ์มหาวิทยาลัย